© 2019. Published by The Company of Biologists Ltd | Journal of Cell Science (2019) 132, jcs226639. doi:10.1242/jcs.226639

RESEARCH ARTICLE

Identification of matrix physicochemical properties required for renal epithelial cell tubulogenesis by using synthetic hydrogels

Ricardo Cruz-Acuña[1,2], Adriana Mulero-Russe[2,3], Amy Y. Clark[2,4], Roy Zent[5] and Andrés J. García[2,4,*]

ABSTRACT

Synthetic hydrogels with controlled physicochemical matrix properties serve as powerful *in vitro* tools to dissect cell–extracellular matrix (ECM) interactions that regulate epithelial morphogenesis in 3D microenvironments. In addition, these fully defined matrices overcome the lot-to-lot variability of naturally derived materials and have provided insights into the formation of rudimentary epithelial organs. Therefore, we engineered a fully defined synthetic hydrogel with independent control over proteolytic degradation, mechanical properties, and adhesive ligand type and density to study the impact of ECM properties on epithelial tubulogenesis for inner medullary collecting duct (IMCD) cells. Protease sensitivity of the synthetic material for membrane-type matrix metalloproteinase-1 (MT1-MMP, also known as MMP14) was required for tubulogenesis. Additionally, a defined range of matrix elasticity and presentation of RGD adhesive peptide at a threshold level of 2 mM ligand density were required for epithelial tubulogenesis. Finally, we demonstrated that the engineered hydrogel supported organization of epithelial tubules with a lumen and secreted laminin. This synthetic hydrogel serves as a platform that supports epithelial tubular morphogenetic programs and can be tuned to identify ECM biophysical and biochemical properties required for epithelial tubulogenesis.

KEY WORDS: Biomaterials, Cell biology, Epithelial morphogenesis, Hydrogel, Synthetic matrix, Tubulogenesis

INTRODUCTION

The extracellular matrix (ECM) provides mechanical and biochemical signals that modulate diverse morphogenetic processes such as renal epithelial morphogenesis (Lelongt and Ronco, 2003; Enemchukwu et al., 2016). For instance, the ECM provides physical support for the three-dimensional (3D) spatial organization of renal epithelial cells into tubular structures. Additionally, interactions between ECM components and integrin receptors regulate mechanotransduction pathways and modulate the activity of signaling molecules (e.g. Wnt family) that mediate the formation of polarized and differentiated epithelia (Lelongt and Ronco, 2003; Liu et al., 2009). In order to understand the contributions of the ECM to epithelial tubulogenesis, 3D collagen gels and Matrigel™ have been used in organotypic cultures that recreate the epithelial morphogenetic developmental program (O'Brien et al., 2002; Lo et al., 2012). In these biological matrices, murine inner medullary collecting duct (IMCD) cells proliferate from single cells to form multicellular tubular or spheroidal structures when cultured in collagen gel or Matrigel™, respectively, recapitulating the morphogenetic program of rudimentary epithelial renal structures (Sakurai et al., 1997; Chen et al., 2004; Rosines et al., 2010; Giles et al., 2014) (Fig. S1A,B). However, these biological matrices are inherently limited by lot-to-lot compositional and structural variability, as well as the inability to decouple biochemical and biomechanical properties (Yu et al., 2005; Hughes et al., 2010). For instance, changes to the bulk concentration (e.g. an increase in matrix density) of collagen gels is a common approach to vary their mechanical properties (Fig. S1C). However, these changes in collagen concentration unavoidably alter other matrix properties, such as adhesive ligand density and fiber density/structure (Cruz-Acuña and García, 2016). Although modulation of bulk concentration of collagen gels results in changes in IMCD-projected area and the longest distance between two points along the projected area (Feret diameter; Fig. S1D,E), it is unknown whether this effect is mediated by differences in biochemical or biomechanical matrix properties between different collagen gel formulations. Furthermore, in the case of Matrigel™, its tumor-derived nature limits its translational potential (Hughes et al., 2010; Cruz-Acuña and García, 2016), establishing a need for a well-defined, tunable biomaterial that recapitulates the role of ECM properties on epithelial morphogenesis with potential for translational therapies. These limitations can be addressed by engineering synthetic hydrogel systems that allow independent control over physicochemical properties and, thus, can be used to dissect the independent contributions of matrix biophysical and biochemical properties to epithelial morphogenesis (Gjorevski et al., 2014, 2016; Cruz-Acuña et al., 2018). These hydrogel systems facilitate the modeling and analysis of cell developmental processes while allowing the dissection of the specific microenvironmental signals that are essential for morphogenesis (Gjorevski et al., 2016; Caliari and Burdick, 2016; Kloxin et al., 2009; Lutolf and Hubbell, 2005), and serve as platforms to model human epithelial developmental programs with clinical translational potential (Gjorevski et al., 2014; Madl et al., 2018; Cruz-Acuña et al., 2017). For example, a synthetic material containing animal-derived heparin, which supports epithelial tubulogenesis programs, has been described as an alternative to biological matrices (Weber et al., 2017).

Here, we describe a fully defined synthetic hydrogel that supports epithelial tubulogenesis of IMCD cells without the use of naturally derived materials. Protease sensitivity, matrix elasticity, and adhesive peptide type and density of the synthetic hydrogel were important parameters in engineering a fully synthetic matrix that supports the IMCD cell tubulogenesis program. The modular design

[1]Wallace H. Coulter Department of Biomedical Engineering, Georgia Institute of Technology, Atlanta, GA 30332, USA. [2]Parker H. Petit Institute for Bioengineering and Biosciences, Georgia Institute of Technology, Atlanta, GA 30332, USA. [3]School of Chemical & Biomolecular Engineering, Georgia Institute of Technology, Atlanta, GA 30332, USA. [4]George W. Woodruff School of Mechanical Engineering, Georgia Institute of Technology, Atlanta, GA 30332, USA. [5]Department of Medicine, Vanderbilt University, Nashville, TN 37235, USA.

*Author for correspondence (andres.garcia@me.gatech.edu)

R.C.-A, 0000-0002-1772-6102; A.Y.C., 0000-0003-4015-1594; A.J.G., 0000-0001-6602-2518

Received 17 October 2018; Accepted 15 September 2019

Journal of Cell Science (2019) 132, jcs226639. doi:10.1242/jcs.226639

of this synthetic matrix allows the study of the independent contributions of physicochemical matrix properties to IMCD cell tubulogenesis and overcomes limitations associated with biological matrices.

RESULTS

PEG-4MAL hydrogel supports MT1-MMP-directed tubule formation in a polymer density-dependent manner

We selected a hydrogel platform based on four-armed maleimide-terminated poly(ethylene glycol) (PEG-4MAL) macromer units that present elements inspired by the ECM, such as cell adhesion peptides and matrix metalloproteinase (MMP)-sensitive crosslinking peptides (Fig. S2A). Although other synthetic hydrogel systems have been developed to mimic properties of biological ECM, the PEG-4MAL hydrogel platform has significant advantages including a well-defined structure, stoichiometric incorporation of bioactive molecules, increased cytocompatibility and improved crosslinking efficiency (Enemchukwu et al., 2016; Caliari and Burdick, 2016; Cruz-Acuña et al., 2017; Phelps et al., 2012; Patterson and Hubbell, 2010). In addition, the tunable properties of PEG-4MAL hydrogels allow the study of the independent contributions of biophysical and biochemical matrix properties for both single and collective epithelial cell programs (Enemchukwu et al., 2016; Cruz-Acuña et al., 2017). For instance, using this platform we have previously shown that normal epithelial cyst growth, polarization and lumen formation for Madin–Darby canine kidney (MDCK) cells are restricted to a narrow range of matrix elasticity, require a threshold level of cell-directed matrix degradability, and are dramatically regulated by adhesive peptide density (Enemchukwu et al., 2016). Therefore, the modular design of this synthetic matrix allows the study of the independent contributions of physicochemical matrix properties to IMCD cell tubulogenesis.

PEG-4MAL macromer was functionalized with adhesive peptide and crosslinked in the presence of IMCD cells to generate cell-encapsulating PEG-4MAL hydrogels (Fig. S2A–C). These synthetic hydrogels were engineered to present a constant 2.0 mM RGD adhesive peptide (GRGDSPC) density and crosslinked with a synthetic peptide containing a protease degradable sequence found in type I collagen (GPQ-W; GCRDGPQGIWGQDRCG). The GPQ-W peptide is predominantly cleaved by MMP1, 2 and 8 (Patterson and Hubbell, 2010), and exhibits low reactivity for MT1-MMP (also known as MMP14) (Turk et al., 2001). The RGD adhesive peptide type and density, and GPQ-W crosslinking peptide have been shown to support MDCK cell viability and cyst morphogenesis in PEG-4MAL hydrogels (Enemchukwu et al., 2016). The mechanical properties of the hydrogel were tuned by varying polymer density (Fig. S2D). Because mechanical ECM properties influence epithelial cell behaviors (Enemchukwu et al., 2016; Cruz-Acuña et al., 2017), we investigated the influence of hydrogel polymer density [5–7% (w/v), 10 kDa PEG-4MAL macromere] on IMCD cell viability and tubule formation (Fig. 1). This combination of macromer size and polymer densities can produce hydrogels with mechanical properties (storage modulus, G′: 500 Pa) that have been shown to support epithelial tubulogenesis (Weber et al., 2017). After 14 days in culture, IMCD cell clusters showed high viability in all hydrogel conditions (Fig. 1A) and a polymer density-dependent effect on both projected area and the longest distance between two points along the projected area (Feret diameter; Fig. 1B–D). At 21 days post-encapsulation, IMCD cell clusters maintained high viability in all hydrogel conditions (Fig. 1E), whereas no tubule formation or cell spreading was observed, and size analysis demonstrated a polymer density-dependent effect on projected area and Feret diameter of the IMCD cell structures (Fig. 1F–H), demonstrating that these PEG-4MAL hydrogel formulations do not support tubulogenesis of IMCD cells.

Considering that proteolytic cleavage of ECM components by MT1-MMPs is essential for renal cell proliferation and tubulogenesis (Lelongt and Ronco, 2003; Riggins et al., 2010), we then examined whether crosslinking of PEG-4MAL hydrogels with a MT1-MMP-sensitive crosslinking peptide supports IMCD cell tubulogenesis. IMCD cells were encapsulated in RGD-functionalized hydrogels of different polymer densities (5–8%, 10 kDa PEG-4MAL) and crosslinked with the MT1-MMP-sensitive crosslinking peptide IPES (GCRDIPESLRAGDRCG) (Patterson and Hubbell, 2010; Turk et al., 2001). These IPES-crosslinked hydrogels exhibited mechanical properties comparable to hydrogels of equal polymer densities but crosslinked with GPQ-W peptide (Fig. S2D). IMCD cells embedded in IPES-crosslinked PEG-4MAL hydrogels maintained high viability at 1 day post-encapsulation in all conditions (Fig. 2A,B). After 5 days in culture, IMCD cells generated cell clusters that showed significant polymer density-dependent effects on cell proliferation, projected area and Feret diameter (Fig. 2C–F). When IMCD cell culture continued for at least 21 days, cell clusters within the 5% and 6% hydrogels developed tubules, as opposed to cells within 7% and 8% hydrogels, which remained as round clusters (Fig. 2G). These results indicate that synthetic hydrogels crosslinked with the IPES peptide support IMCD tubulogenesis, likely due to its specificity for MT1-MMP as compared to collagen-derived peptides (e.g. GPQ-W) (Patterson and Hubbell, 2010; Turk et al., 2001). Furthermore, polymer density has a significant effect on IMCD cell proliferation, multi-cellular growth and tubule formation. Although 5% PEG-4MAL hydrogels supported tubule formation, this formulation was less likely to endure experimental handling compared to 6% PEG-4MAL hydrogels by 21 days in culture. We therefore selected 6.0% (10 kDa) PEG-MAL hydrogels crosslinked with the MT1-MMP-sensitive IPES crosslinker for subsequent studies.

Adhesive peptide type directs tubule formation

Cell adhesion receptor interactions with ECM components provide signals critical for cell survival, proliferation and tubulogenesis (Chen et al., 2004; Cruz-Acuña and García, 2016; Wickström et al., 2011; Hynes, 2002; Giancotti and Ruoslahti, 1999; Adams and Watt, 1993). Therefore, we examined whether the adhesive peptide type in the synthetic hydrogel impacts IMCD tubule formation. IMCD cells were embedded within 6% PEG-4MAL (10 kDa) hydrogels crosslinked with a constant IPES density and functionalized with different cysteine-terminated adhesive peptides (all at 2.0 mM; Fig. 3), namely, RGD, inactive scrambled peptide RDG (GRDGSPC), type I collagen-mimetic triple helical GFOGER [GYGGGP(GPP)$_5$GFOGER(GPP)$_5$GPC] (Emsley et al., 2004) and laminin β1 chain-derived YIGSR (CGGEGYGEGYIGSR) (Kikkawa et al., 2014). IMCD cells encapsulated in RGD-functionalized hydrogels exhibited the highest level of proliferation (Fig. 3A,B) and showed significant increases in projected area and Feret diameter as compared to GFOGER- or YIGSR-functionalized hydrogels at 5 days post-encapsulation (Fig. 3C,D). Additionally, IMCD cells encapsulated in PEG-4MAL hydrogels functionalized with inactive RDG peptide showed significant reductions in cell proliferation when compared to RGD (Fig. 3A,B) and smaller cluster size compared to other hydrogel conditions (Fig. 3C,D). Furthermore, at 21 days post-

Journal of Cell Science (2019) 132, jcs226639. doi:10.1242/jcs.226639

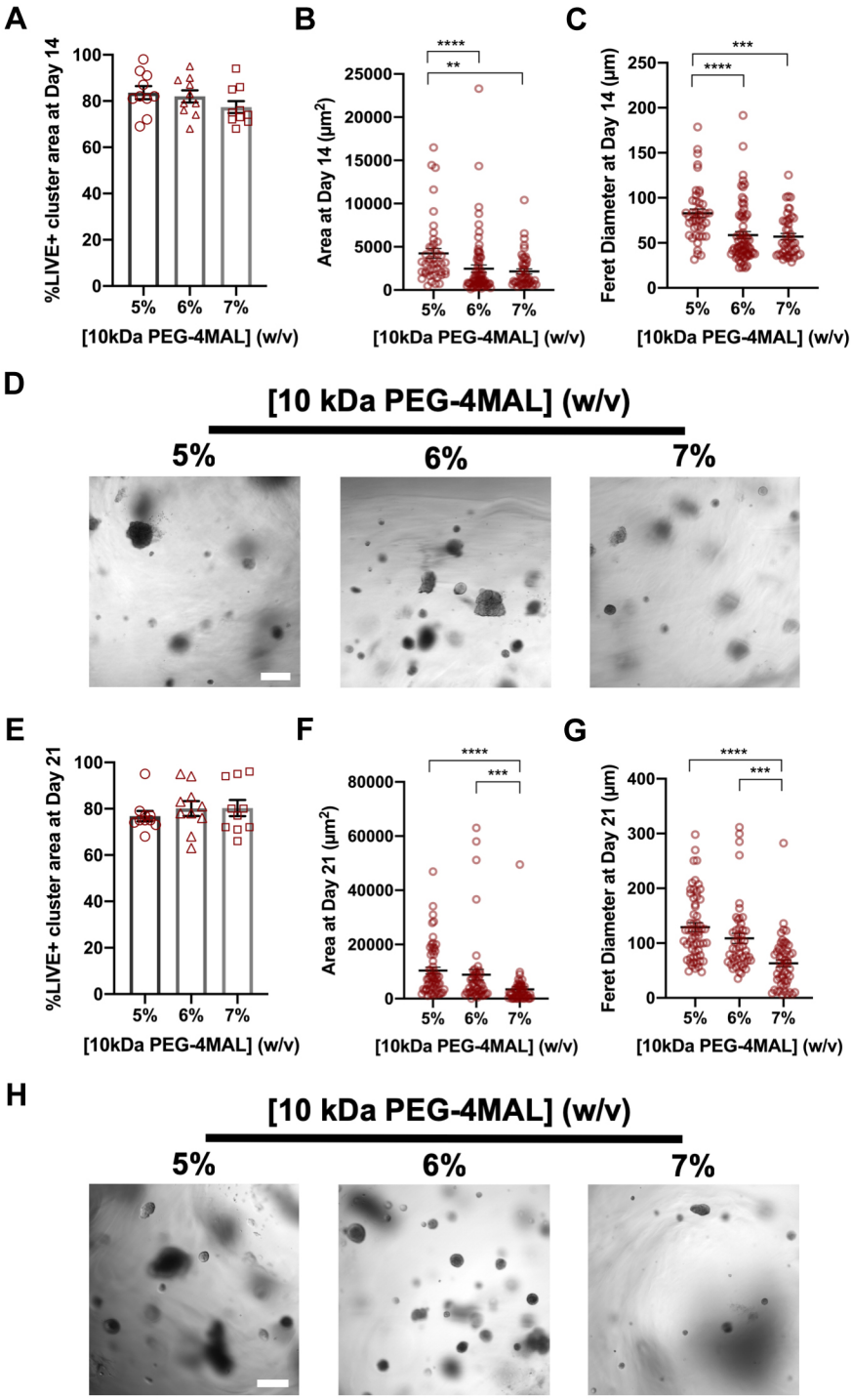

Fig. 1. PEG-4MAL hydrogel crosslinked with GPQ-W peptide does not support tubule formation. (A) Percentage of IMCD cluster area that stained for LIVE (C_{12}-Resazurin) after 14 days of encapsulation in PEG-4MAL hydrogels of different polymer density and crosslinked with GPQ-W peptide (mean±s.e.m.). IMCD multicellular structure (B) projected area and (C) Feret diameter at 14 days after encapsulation in PEG-4MAL hydrogel. (D) Transmitted light images of IMCD cells cultured in PEG-4MAL hydrogels. Scale bar: 100 µm. (E) Percentage of IMCD cluster area that stained for LIVE after 21 days of encapsulation in PEG-4MAL hydrogels (mean±s.e.m.). IMCD multicellular structure (F) projected area and (G) Feret diameter at 21 days after encapsulation in PEG-4MAL hydrogels. (H) Transmitted light images of IMCD cells at 21 days after encapsulation in PEG-4MAL hydrogels. Scale bar: 200 µm. Graph lines represent the mean of the individual data points. Each data point represents one multicellular structure. ****P<0.0001, ***P<0.0002, **P<0.0021 (Kruskal–Wallis with Dunn's multiple comparisons test). Experiments performed with six PEG-4MAL hydrogels per experimental group. Four independent experiments were performed and data are presented for one of the experiments.

encapsulation, IMCD cell tubule formation was observed in the RGD and GFOGER gel formulations, whereas cells encapsulated in RDG or YIGSR-functionalized hydrogels did not generate tubules (Fig. 3E,F). These results show an adhesive peptide type-dependent effect on tubulogenesis of IMCD cells after 21 days in culture. We note that different synthetic peptides promote differences in cell responses within ECM-derived substrates (Livant et al., 2000), which may ultimately contribute to the differences in cluster size and tubulogenesis observed among groups. For instance, fibronectin-derived peptides (e.g. RGD), in addition to increasing cell migration, augment integrin signaling (Miyamoto et al., 1995) and can induce expression of proteases, facilitating cell invasion (Werb et al., 1989; Lash et al., 1987), and potentially influencing IMCD cluster size and tubulogenesis. As RGD-functionalized hydrogels supported the highest level of cell proliferation, and significant growth compared to other adhesive peptides, we used RGD-functionalized hydrogels for subsequent studies.

PEG-4MAL macromer size promotes early tubulogenesis

Because previous studies have suggested that matrix elasticity influences epithelial cell behaviors (Enemchukwu et al., 2016; Cruz-Acuña et al., 2017), we investigated the influence of a lower

Journal of Cell Science (2019) 132, jcs226639. doi:10.1242/jcs.226639

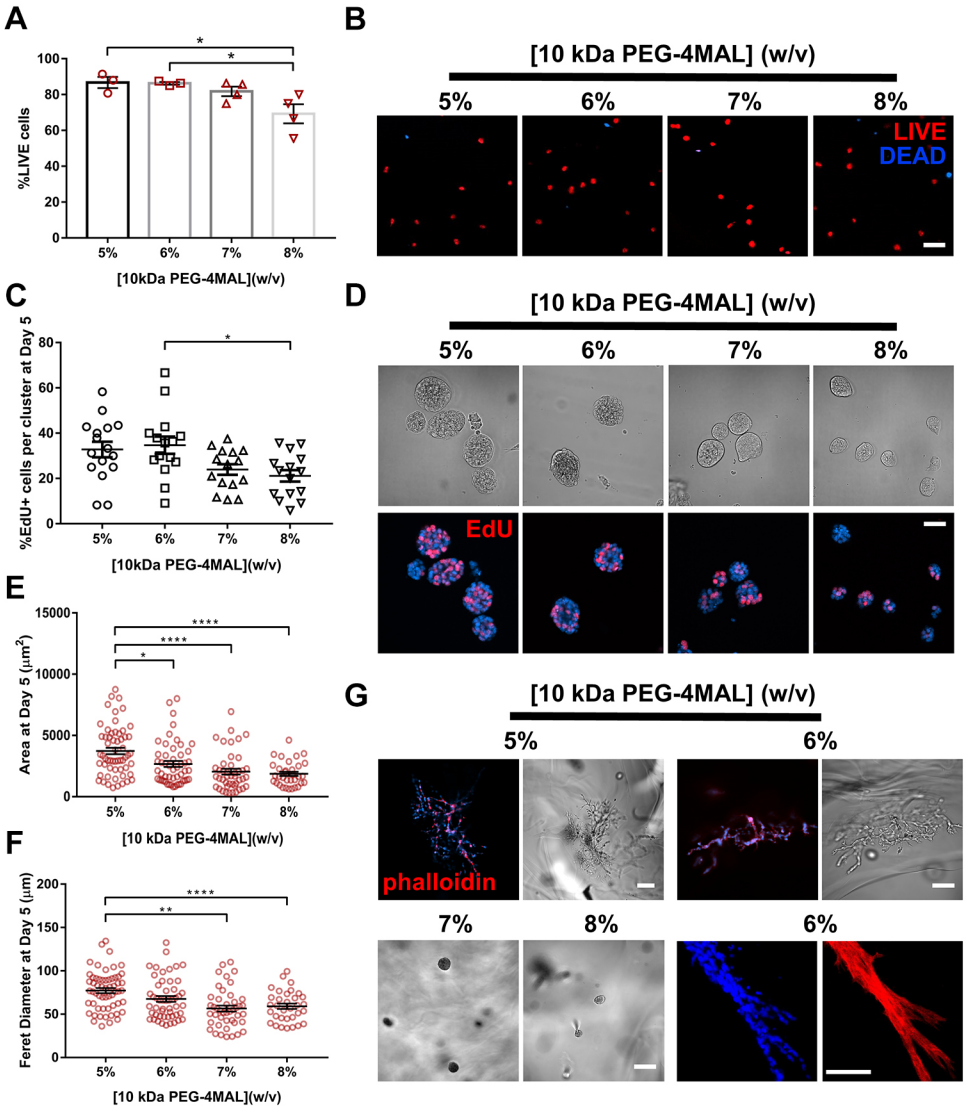

Fig. 2. Polymer density of 10 kDa PEG-4MAL directs tubule formation. (A) Percentage of IMCD cells that stained for LIVE (C_{12}-Resazurin) after 1 day of encapsulation in 10 kDa PEG-4MAL hydrogels of different polymer density (mean±s.e.m.). Each data point represents one hydrogel sample. At least 100 cells were assessed per condition. (B) Fluorescence microscopy images of IMCD cells cultured in PEG-4MAL hydrogels of different polymer density. IMCD cell viability was assessed at 1 day after encapsulation. Scale bar: 100 µm. (C) Percentage of IMCD cells per cluster that were labeled by EdU incorporation (mean±s.e.m.) after 5 days of encapsulation. At least 30 clusters were analyzed per condition. (D) Transmitted light and fluorescence microscopy images of proliferating (EdU+) IMCD cells cultured in PEG-4MAL hydrogels of different polymer density. IMCD cell proliferation was assessed at 5 days after encapsulation. Scale bar: 50 µm. IMCD multicellular structure (E) projected area and (F) Feret diameter at 5 days after encapsulation in PEG-4MAL hydrogel. Graph line represents the mean of the individual data points. Each data point represents one multicellular structure. (G) Transmitted light and fluorescence microscopy images of IMCD cells at 21 days after encapsulation in PEG-4MAL hydrogel and labeled for actin (phalloidin). DAPI was used as a counterstain. Scale bars: 100 µm. ****P<0.0001, **P<0.001, *P<0.0332 (Kruskal–Wallis with Dunn's multiple comparisons test). Experiments performed with six PEG-4MAL hydrogels per experimental group. Three independent experiments were performed and data are presented for one of the experiments.

range of matrix elasticity on IMCD cell viability, proliferation and tubule formation. As changes in PEG-4MAL macromer size and polymer density modulate hydrogel elasticity and permeability (Enemchukwu et al., 2016; Cruz-Acuña et al., 2017), IMCD cells were encapsulated in hydrogels of 20 kDa macromer size and a range of polymer densities [8–14% (w/v)] that exhibit a lower range of matrix elasticity (Fig. S2E) compared to 10 kDa PEG-4MAL hydrogels (Fig. S2D). The synthetic hydrogels were functionalized with the adhesive peptide RGD and crosslinked using the MT1-MMP-sensitive IPES peptide. No differences in cell viability were observed in any of the hydrogel conditions at 1 day post-encapsulation (Fig. 4A,B), whereas IMCD cell proliferation, projected area and Feret diameter varied in a polymer density-dependent manner at 5 days post-encapsulation (Fig. 4C–F). Moreover, as early as 7 days after encapsulation, cell sprouting was observed in the 8% hydrogel whereas round cell clusters continued to develop in all other hydrogel formulations (Fig. 4G). By 14 days of culture in the synthetic matrix, tubule formation was observed in a polymer density-dependent manner, where the 8% PEG-4MAL hydrogel had a higher number of cell structures presenting tubules, whereas significantly less tubule formation was observed in the higher (12% and 14%) polymer density conditions (Fig. 5A). IMCD cells formed multicellular structure phenotypes classified as: (1) 'smooth clusters', which are smooth-contoured, spherical-like aggregates; (2) 'spiked clusters', which are aggregates characteristically decorated by numerous thin cytoplasmic processes extending out radially from the bulk of the IMCD cluster into the surrounding matrix, in contrast to the smooth-contoured appearance of the 'smooth clusters'; or (3) 'tubules', which are aggregates characteristically decorated by numerous cellular processes extending out into the surrounding matrix and forming a complex network of branching cords extending out from the initial processes, in accordance with previous reports (Weber et al., 2017; Montesano et al., 1991) (Fig. S3). Evaluation of the distribution of cell cluster morphologies showed a higher frequency of tubule formation in 8%, 20 kDa hydrogels compared to other hydrogel conditions (Fig. 5B). Further analysis of the Feret diameter of tubule-presenting cell structures demonstrated a significantly higher length of tubules in the 8%, 20 kDa PEG-4MAL hydrogels as compared to tubules formed in 6%, 10 kDa hydrogels (Fig. 5C). These results demonstrate that IMCD cell encapsulation in PEG-4MAL hydrogels of 20 kDa macromer size resulted in cell spreading and tubule formation at an earlier time point and with an increased length of tubules, when compared to IMCD tubules

Journal of Cell Science (2019) 132, jcs226639. doi:10.1242/jcs.226639

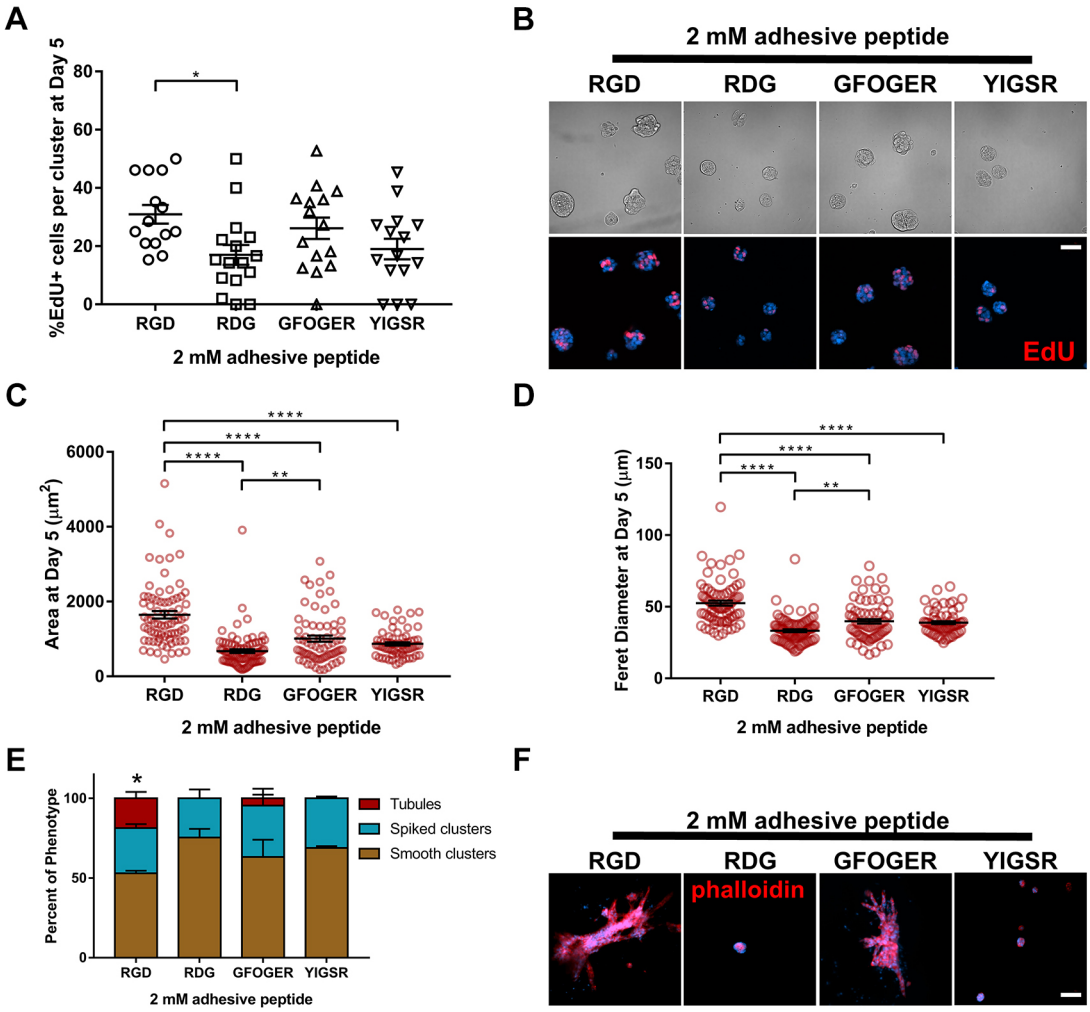

Fig. 3. Adhesive peptide type in PEG-4MAL hydrogels directs tubule formation. (A) Percentage of IMCD cells per cluster that were labeled by EdU incorporation (mean±s.e.m.) after 5 days of encapsulation in PEG-4MAL hydrogels functionalized with different adhesive peptides. At least 30 clusters were analyzed per condition. (B) Transmitted light and fluorescence microscopy images of proliferating (EdU+) IMCD cells cultured in PEG-4MAL hydrogels functionalized with different adhesive peptides. IMCD cell proliferation was assessed at 5 days after encapsulation. Scale bar: 50 µm. IMCD multicellular structure (C) projected area and (D) Feret diameter at 5 days after encapsulation in PEG-4MAL hydrogel. Graph line represents the mean of the individual data points. Each data point represents one multicellular structure. (E) Percentage of IMCD multicellular structures (mean±s.e.m.) that were classified as either 'smooth clusters', 'spiked clusters' or 'tubules' after 21 days of encapsulation. At least 10 multicellular structures were analyzed per condition. (F) Fluorescence microscopy images of IMCD cells at 21 days after encapsulation in PEG-4MAL hydrogel and labeled for actin (phalloidin). DAPI, counterstain. Scale bar: 50 µm. **P*<0.0332, ***P*<0.0021, *****P*<0.0001 (A,C,D); **P*<0.0002 for RGD versus RDG and *P*<0.0021 for RGD versus YIGSR (E). (A,C,D, Kruskal–Wallis with Dunn's multiple comparisons test; E, χ^2 test with Bonferroni's correction). Experiments performed with six PEG-4MAL hydrogels per experimental group. Three independent experiments were performed and data are presented for one of the experiments.

formed in synthetic hydrogels prepared with the 10 kDa macromer (Figs 2, 4 and 5). The strong dependence of IMCD multicellular growth and tubulogenesis on hydrogel polymer density and macromer size suggests that tubule formation is regulated by hydrogel elasticity. However, changes in polymer density and macromer size also alter hydrogel permeability (Enemchukwu et al., 2016). Although it is not possible to uncouple mechanical properties from diffusional properties over the range of polymer densities examined in this study, we have previously shown that viability, growth and morphogenesis of different epithelial systems within RGD-functionalized PEG-4MAL hydrogels is independent from differences in permeability (Enemchukwu et al., 2016; Cruz-Acuña et al., 2017). This result suggests that polymer density- or macromer size-dependent IMCD cell tubulogenesis is related to hydrogel mechanical properties; however, changes on IMCD tubulogenesis due to differences in permeability between PEG-4MAL macromers cannot be completely ruled out. Additional experiments revealed that, by 7 days post-encapsulation, cell viability was compromised in softer (6%, 20 kDa; Fig. S4A) and in GPQ-W-crosslinked (8%, 20 kDa; Fig. S4B) PEG-4MAL hydrogels, as compared to that in 8%, 20 kDa PEG-4MAL hydrogels (Fig. S4C). Additionally, IMCD cells encapsulated in (8% 20 kDa) hydrogels crosslinked with a non-degradable molecule (hexa(ethylene glycol) dithiol; PEGDT) exhibited significantly lower viability and smaller cluster size (area and Feret diameter) at 3 days and 11 days post-encapsulation, respectively, as compared to cells in IPES-crosslinked hydrogels (Fig. S4D–G), showing that the survival and growth of IMCD structures are dependent on a degradable matrix. Therefore, we designated 8% 20 kDa PEG-4MAL crosslinked with IPES as the synthetic polymer density, macromer size and crosslinker that provides the physical support and biomechanical signals necessary

Journal of Cell Science (2019) 132, jcs226639. doi:10.1242/jcs.226639

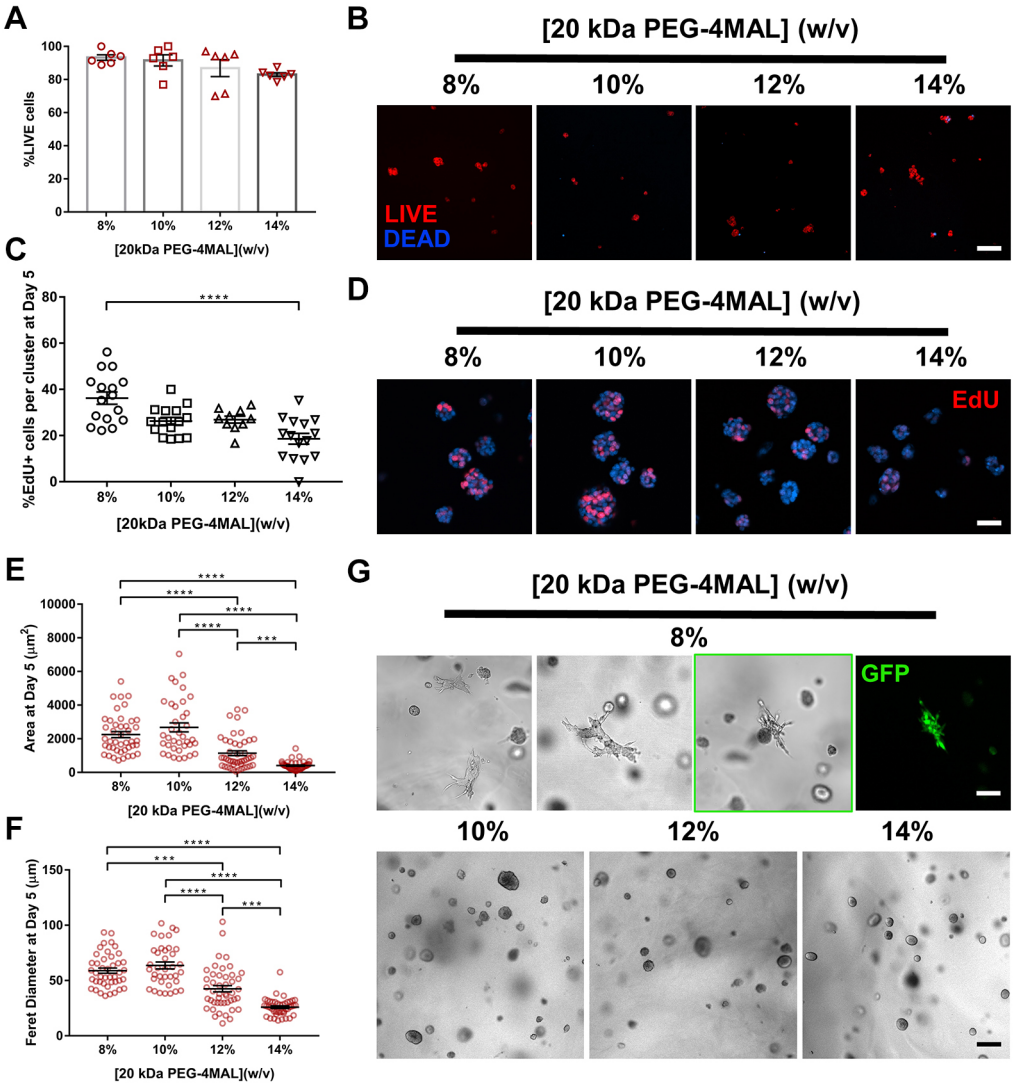

Fig. 4. Polymer density of 20 kDa PEG-4MAL directs tubule formation. (A) Percentage of IMCD cells that stained for LIVE (C_{12}-Resazurin) after 1 day of encapsulation in 20 kDa PEG-4MAL hydrogels of different polymer density (mean±s.e.m.). Each data point represents one independent hydrogel. At least 100 cells were assessed per condition. (B) Fluorescence microscopy images of IMCD cells cultured in PEG-4MAL hydrogels of different polymer density. IMCD cell viability was assessed at 1 day after encapsulation. Scale bar: 50 µm. (C) Percentage of IMCD cells per cluster that were labeled by EdU incorporation (mean ±s.e.m.) after 5 days of encapsulation. At least 30 clusters were analyzed per condition. (D) Fluorescence microscopy images of proliferating (EdU+) IMCD cells cultured in PEG-4MAL hydrogels of different polymer density. IMCD cell proliferation was assessed at 5 days after encapsulation. Scale bar: 50 µm. IMCD multicellular structure (E) projected area and (F) Feret diameter at 5 days after encapsulation in PEG-4MAL hydrogel. Graph line represents the mean of the individual data points. Each data point represents one multicellular structure. (G) Transmitted light and fluorescence microscopy images of IMCD cells at 7 days after encapsulation in PEG-4MAL hydrogel. Scale bars: 100 µm for 8% and 200 µm for other conditions. ****P<0.0001, ***P<0.0002 (Kruskal–Wallis with Dunn's multiple comparisons test). Experiments performed with six PEG-4MAL hydrogels per experimental group. Three independent experiments were performed and data are presented for one of the experiments.

for optimal IMCD cell growth and tubule formation within PEG-4MAL hydrogels.

Adhesive peptide density in PEG-4MAL hydrogels regulates tubule formation

We next examined the effects of RGD adhesive peptide density on tubulogenesis within PEG-4MAL hydrogels engineered to present optimal biochemical properties (8%, 20 kDa PEG-4MAL). A total density (2.0 mM) of a mixture of cell-adhesive RGD peptide and scrambled inactive RDG peptide was used to vary RGD density (0.4–2.0 mM) while maintaining identical structures among hydrogel formulations and constant IPES crosslinking peptide density (Fig. 6). Additionally, a hydrogel condition with a total RGD density of 4.0 mM (9.15%, 20 kDa) was used while preserving equal IPES crosslinking peptide density and mechanical properties (Fig. S2E; Fig. 6). Cell viability and proliferation at 1 and 5 days post-encapsulation, respectively, was insensitive to RGD peptide density (Fig. 6A–D). However, cluster area and Feret diameter showed a significant dependence on RGD density at 5 days post-encapsulation (Fig. 6E,F). Hydrogels presenting low (<2.0 mM) RGD densities supported the formation of relatively small multicellular structures with no significant differences among the groups (0.4, 1.0 and 1.6 mM RGD; Fig. 6E,F). In contrast, hydrogels presenting high (≥2.0 mM) RGD density formed larger structures with no statistical differences between these groups (2.0 and 4.0 mM RGD; Fig. 6E,F). Further

Journal of Cell Science (2019) 132, jcs226639. doi:10.1242/jcs.226639

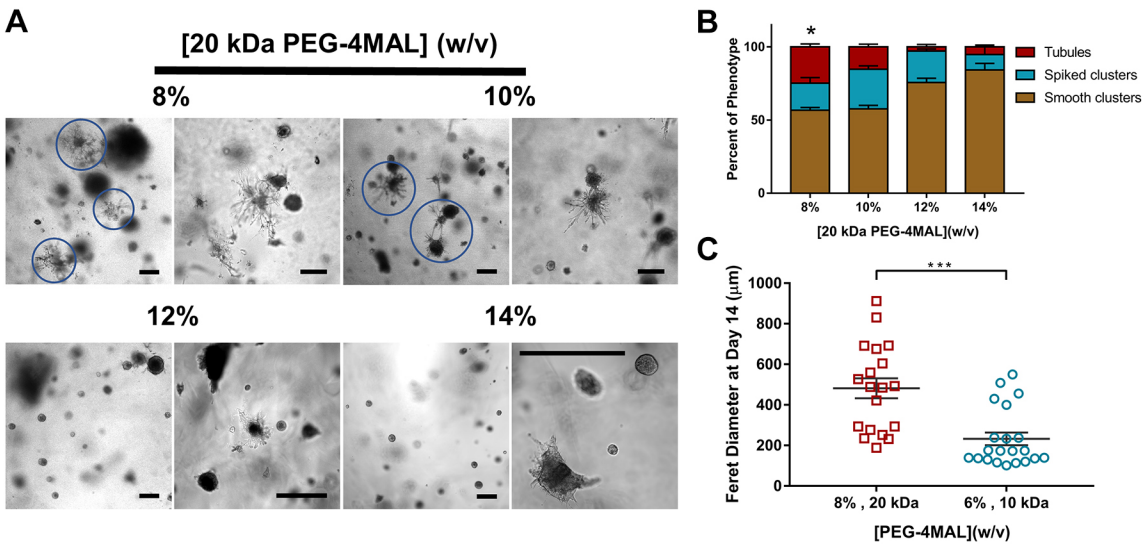

Fig. 5. Polymer density and macromer size controls tubule formation. (A) Transmitted light images of IMCD cells cultured in 20 kDa PEG-4MAL hydrogels of different polymer density at 14 days after encapsulation. Scale bar: 200 µm. (B) Percentage of IMCD multicellular structures (mean±s.e.m.) that were classified as either 'smooth clusters', 'spiked clusters' or 'tubules' after 21 days of encapsulation. At least 10 multicellular structures were analyzed per condition. **P*<0.0001 for 8% versus 12% and *P*<0.0002 for 8% versus 14% (χ^2 test with Bonferroni's correction). (C) IMCD multicellular structure Feret diameter at 14 days after encapsulation in PEG-4MAL hydrogels of different macromer size. Graph line represents the mean of the individual data points. Each data point represents one multicellular structure. ****P*<0.0002 (unpaired *t*-test with Welch's correction). Experiments performed with six PEG-4MAL hydrogels per experimental group. Three independent experiments were performed and data are presented for one of the experiments.

analysis of cellular structures at 14 days post-encapsulation demonstrated a RGD density-dependent effect on the frequency and Feret diameter of tubule-presenting cell structures (Fig. 6G–I). No significant differences were observed between the two high RGD density (2 and 4 mM) hydrogels. EdU staining of emerging tubules at 14 days post-encapsulation revealed that cell proliferation is not higher in emerging tubules than in the bulk of the multicellular cluster (Fig. 6J), suggesting that cell proliferation is not the only factor contributing to tubule formation. Together, these results are consistent with previous studies showing that adhesive ligand density regulates epithelial morphogenesis independently of cell proliferation (Enemchukwu et al., 2016), and suggest that high RGD density may support formation of longer tubules within the synthetic hydrogels by promoting increased integrin-mediated cell migration and/or increased cell–cell contacts via α-catenin activation. Given that differences in the level of cell proliferation exist among IMCD clusters within the same hydrogel condition, it is important to note that these observations are based on a population level analysis and do not necessarily describe individual cell clusters. Taken together, these results identify an engineered hydrogel formulation (storage modulus, G′: 200 Pa; 8% polymer density; 20 kDa macromer size; 2.0 mM RGD adhesive peptide; IPES crosslinking peptide) that supports IMCD viability and optimized cell proliferation, growth and formation of tubules.

Engineered hydrogel supports key features of IMCD cell tubule differentiation

The IMCD cell tubulogenesis program is characterized by the 3D assembly of epithelial cells into tubules and formation of a differentiated epithelium (Lelongt and Ronco, 2003). Interactions between laminin and integrin receptors are required for renal epithelial differentiation (Lelongt and Ronco, 2003; Liu et al., 2009; Chen et al., 2004; Zent et al., 2001; Zhang et al., 2009). Therefore, to further characterize IMCD tubule differentiation, we examined laminin secretion and the role of integrin receptors of IMCD cell tubules generated within the engineered synthetic matrix. Over 21 days in culture, the engineered synthetic hydrogel supported a substantial increase in the number of multicellular structures forming organized tubules over time (Fig. S5A,B). Furthermore, the hydrogel-generated IMCD tubules demonstrated an organized tubular assembly with a lumen (Fig. 7A–C), and secretion of laminin into the basal side of the tubular structures (Lelongt and Ronco, 2003; Riggins et al., 2010) (Fig. 7D,E). We next evaluated the role of integrin receptors and mediators of mechanotransduction pathways on the IMCD cell tubulogenesis program within the engineered hydrogel. Previous studies have demonstrated that the IMCD cell morphogenesis program requires sequential cell adhesion to ECM via laminin ($\alpha_3\beta_1$)- and collagen ($\alpha_1\beta_1$ and $\alpha_2\beta_1$)-binding integrins, which promote cell spreading, proliferation and migration, to ultimately form multicellular tubular structures (Lelongt and Ronco, 2003; Chen et al., 2004; Zhang et al., 2009). Addition of blocking antibodies against α_1, α_2 and β_1 integrin subunits to IMCD culture resulted in significant reductions in tubule formation at 21 days post-encapsulation as compared to control group (DMSO; Fig. S5C,D). Additionally, treatment with blebbistatin or Y-27632, which inhibit myosin II and the Rho-associated kinases (Straight et al., 2003; Uehata et al., 1997), respectively, resulted in significant reductions in tubule formation (Fig. S5C,D), indicating that cellular contractility is important to IMCD tubulogenesis.

Finally, as previous studies have shown that MTI-MMP proteolytic activity is required for renal epithelial branching tubulogenesis in biological matrices as early as 3 days post-encapsulation (Riggins et al., 2010; Pohl et al., 2000), we further assessed MT1-MMP-mediated tubulogenesis of IMCD cells within engineered PEG-4MAL hydrogels. We incubated IMCD cells in a blocking antibody specific to the catalytic domain of MT1-MMP (AB6005) starting at 3 days post-encapsulation in the engineered hydrogel, and demonstrated reduced tubule formation after 15 days

Journal of Cell Science (2019) 132, jcs226639. doi:10.1242/jcs.226639

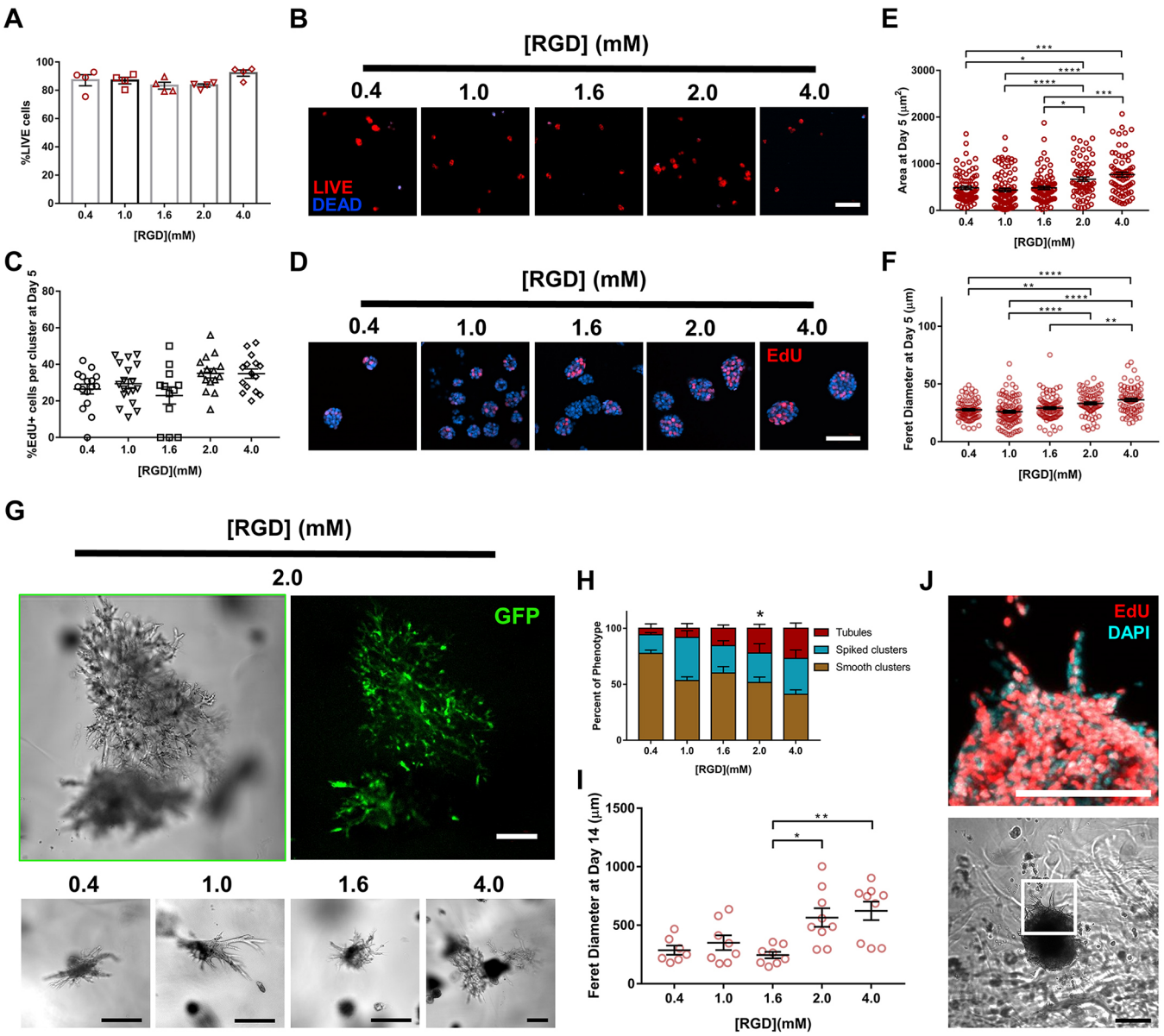

Fig. 6. Adhesive peptide density in PEG-4MAL hydrogels regulates tubule formation. (A) Percentage of IMCD cells that stained for LIVE (C_{12}-Resazurin) after 1 day of encapsulation in 8%, 20 kDa PEG-4MAL hydrogels functionalized with varying RGD density and crosslinked with IPES peptide (mean±s.e.m.). Each data point represents one independent hydrogel. At least 100 cells were assessed per condition. (B) Fluorescence microscopy images of IMCD cells cultured in PEG-4MAL hydrogel. IMCD cell viability was assessed at 1 day after encapsulation. Scale bar: 50 µm. (C) Percentage of IMCD cells per cluster that were labeled by EdU incorporation (mean±s.e.m.) after 5 days of encapsulation. At least 30 clusters were analyzed per condition. (D) Fluorescence microscopy images of proliferating (EdU+) IMCD cells cultured in PEG-4MAL hydrogels of different polymer density. IMCD cell proliferation was assessed at 5 days after encapsulation. Scale bar: 50 µm. IMCD multicellular structure (E) projected area and (F) Feret diameter at 5 days after encapsulation in PEG-4MAL hydrogel. Graph line represents the mean of the individual data points. Each data point represents one multicellular structure. (G) Transmitted light and fluorescence microscopy images of GFP-expressing IMCD cells at 14 days after encapsulation in PEG-4MAL hydrogel. Scale bars: 100 µm. (H) Percentage of IMCD multicellular structures (mean±s.e.m.) that were classified as 'smooth clusters', 'spiked clusters' or 'tubules' after 14 days of encapsulation. At least 10 multicellular structures were analyzed per condition. *P<0.0021 for 2.0 versus 0.4 mM RGD (χ^2 test with Bonferroni's correction). (I) IMCD multicellular structure Feret diameter at 14 days after encapsulation in PEG-4MAL hydrogel. Graph line represents the mean of the individual data points. Each data point represents one multicellular structure. ****P<0.0001, ***P<0.0002, **P<0.0021, *P<0.0332 (Kruskal–Wallis with Dunn's multiple comparisons test). (J) Transmitted light and fluorescence microscopy images (magnification of boxed area) of proliferating (EdU+) IMCD cells cultured in PEG-4MAL hydrogels functionalized with 2.0 mM RGD. Scale bars: 100 µm. Experiments performed with six PEG-4MAL hydrogels per experimental group. Three independent experiments were performed and data are presented for one of the experiments.

of culture, compared with the vehicle-only (DMSO) control (Fig. 8A,B). Additionally, IMCD cell culture revealed an increased expression of MT1-MMP at the cell–hydrogel interface at the multicellular and single-cell level (Fig. 8C), suggesting that MT1-MMP acts at the cell surface to remodel the synthetic hydrogel matrix. Taken together, these results demonstrate that the engineered PEG-4MAL hydrogel robustly supports key features of tubular differentiation of IMCD cells. Additionally, these results provide preliminary indication that IMCD tubulogenesis in the synthetic matrix is also directed by cell receptor interactions with

Journal of Cell Science (2019) 132, jcs226639. doi:10.1242/jcs.226639

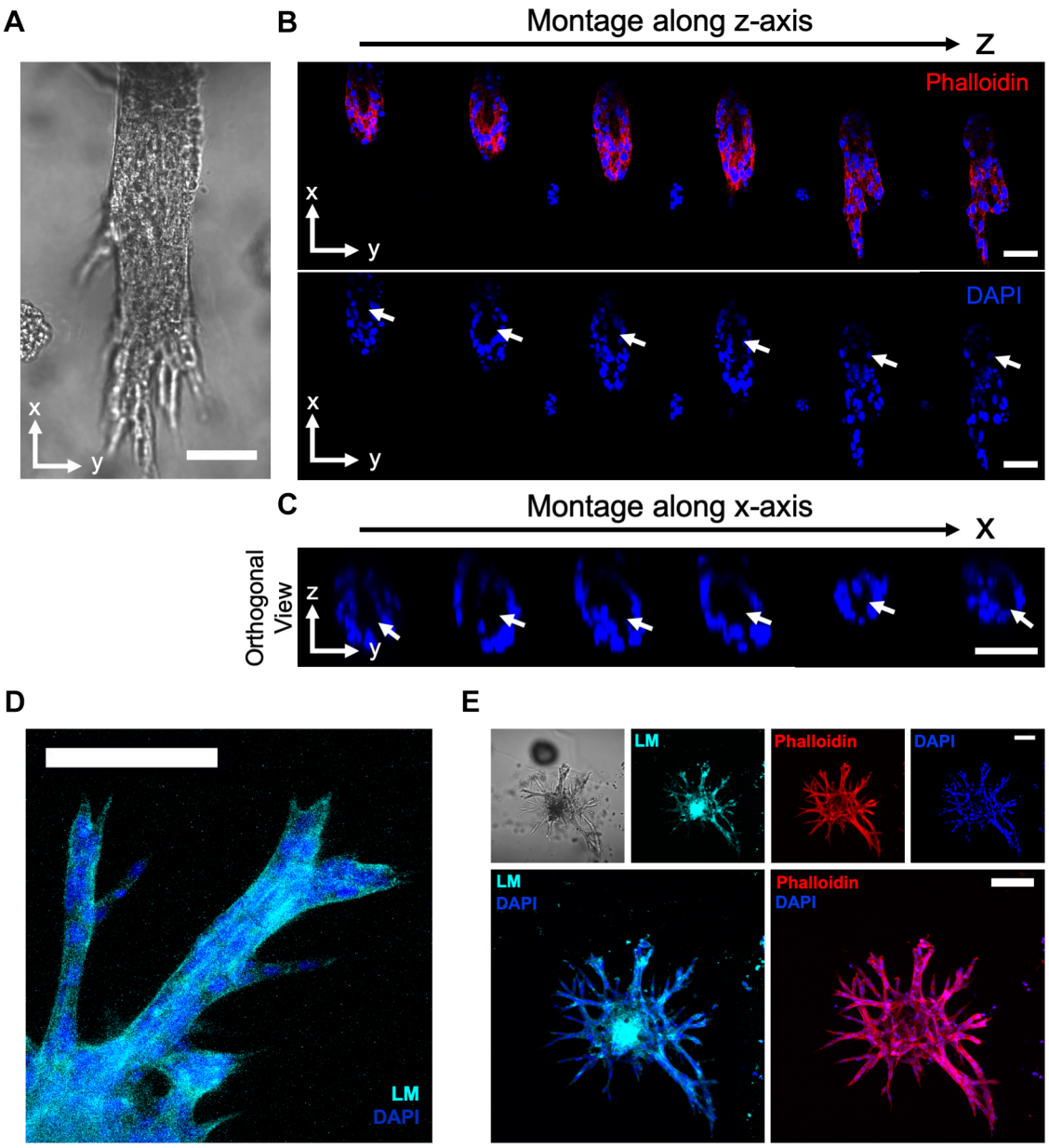

Fig. 7. Engineered PEG-4MAL hydrogel promotes key features of epithelial tubule differentiation. (A–C) Transmitted light and fluorescence microscopy images of a lumenized IMCD tubule within engineered hydrogel stained for actin (phalloidin) and nuclei (DAPI). White arrows show the lumen. Scale bars: 50 µm. (D) Fluorescence microscopy image of IMCD tubules within engineered hydrogel stained for secreted laminin (LM). Scale bar: 100 µm. (E) Transmitted light and fluorescence microscopy images of IMCD tubules within engineered hydrogel stained for LM, actin (phalloidin) and nuclei (DAPI). Scale bars: 100 µm. Experiments performed with six PEG-4MAL hydrogels per experimental group. Three independent experiments were performed and data are presented for one of the experiments.

secreted laminin, cellular contractility and MT1-MMP activity at initial stages of tubule development.

PEG-4MAL hydrogel supports tubulogenesis of other kidney epithelial cells

To determine whether the synthetic hydrogel can be used to study epithelial tubulogenesis of other kidney epithelial cells, murine renal proximal tubule cells (RPTCs) were cultured in 6% and 10% 20 kDa PEG-4MAL hydrogels functionalized with 2.0 mM RGD adhesive peptide and crosslinked with IPES peptide. RPTCs showed high viability in both conditions at 1 day post-encapsulation, with no significant differences between the groups (Fig. S6A). After 28 days in culture, RPTC tubule formation was observed in the 10% hydrogel condition, whereas no tubule formation was observed in 6% hydrogels. Analysis of the Feret diameter of RPTC multicellular structures demonstrated formation of significantly larger structures in the 10% hydrogel as compared to 6% hydrogel (Fig. S6B,C). These results establish PEG-4MAL hydrogels as a tunable platform that supports tubulogenesis of different kidney epithelial cell systems.

DISCUSSION

This research describes a fully-defined synthetic hydrogel with independent control over its proteolytic degradation, mechanical properties, and adhesive ligand type and density that serves as a modular platform to study the impact of biochemical and

Journal of Cell Science (2019) 132, jcs226639. doi:10.1242/jcs.226639

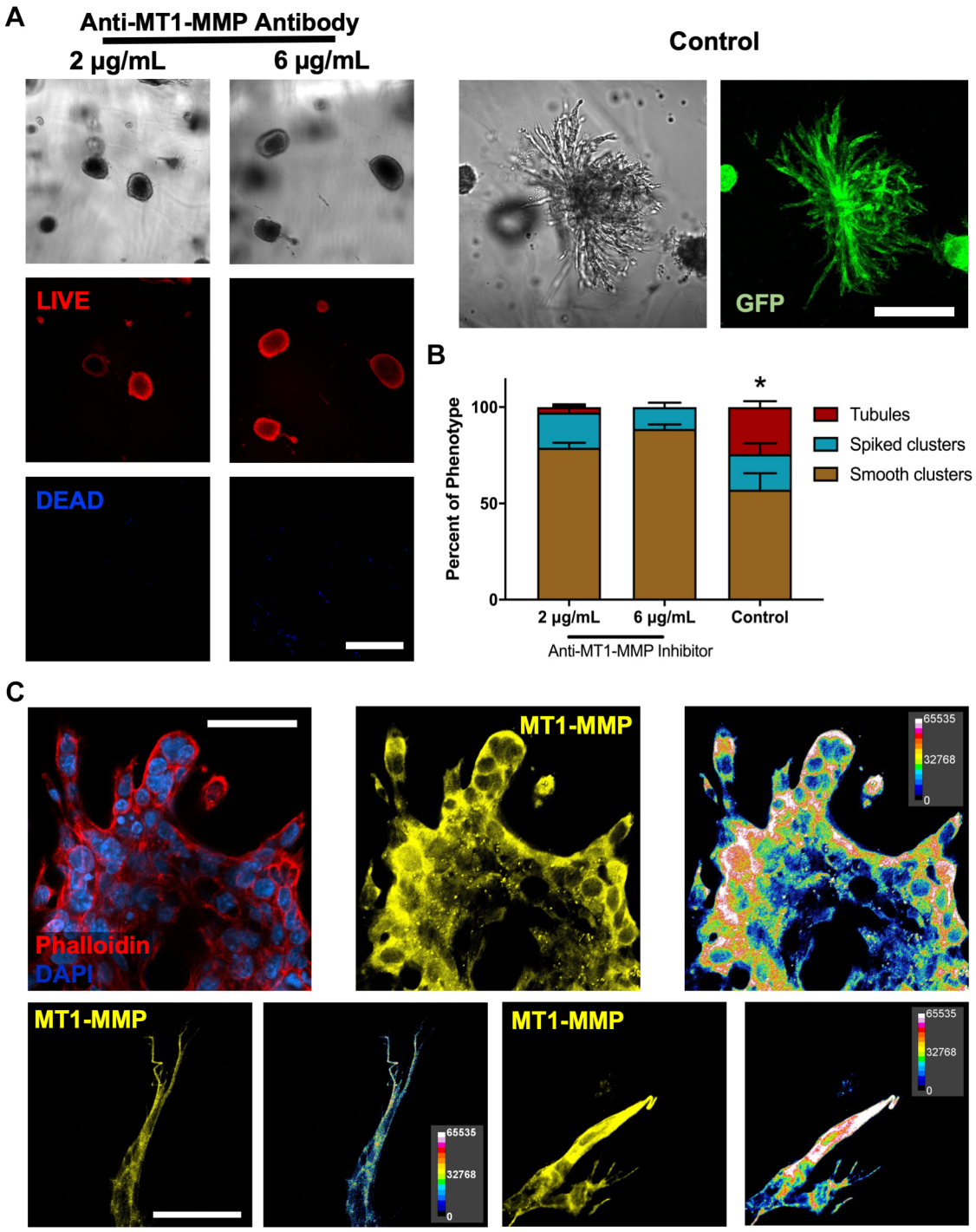

Fig. 8. PEG-4MAL hydrogels support MMP-mediated tubule formation. (A) Transmitted light and fluorescence microscopy images of IMCD cells cultured within engineered PEG-4MAL hydrogel and in the presence of an MT1-MMP inhibitor (anti-MT1-MMP antibody) or vehicle control (0.05% sodium azide). IMCD cell viability was assessed at 15 days after encapsulation. Scale bars: 200 µm. (B) Percentage of IMCD multicellular structures (mean±s.e.m.) that were classified as 'smooth clusters', 'spiked clusters' or 'tubules' after 15 days of encapsulation. At least 10 multicellular structures were analyzed per condition. (C) Fluorescence microscopy images of IMCD cells cultured within engineered PEG-4MAL hydrogel stained for actin (phalloidin), nuclei (DAPI) and expression of MT1-MMP. Relative fluorescence intensity analysis was performed on MT1-MMP images. Scale bars: 50 µm. *P<0.0001 for control versus 2 µg/ml, and control versus 6 µg/ml anti-MT1-MMP antibody (χ^2 test with Bonferroni's correction). Experiments performed with six PEG-4MAL hydrogels per experimental group. Three independent experiments were performed and data are presented for one of the experiments.

mechanical matrix properties on epithelial tubular morphogenesis. Systematic changes in hydrogel formulation to independently tune hydrogel macromer size and polymer density, adhesive ligand type and density, and MMP-dependent degradation revealed that each of these properties has profound effects on this coordinated multicellular morphogenetic process, including cell viability, proliferation and tubular structure development. Additionally, we identified an engineered synthetic hydrogel formulation that

promotes lumenized tubule formation, integrin- and MT1-MMP-mediated growth of tubules, and supports increases in the number and length of tubules over time. These new observations are not attainable when using biological ECMs due to the experimental inability to decouple matrix biochemical and mechanical properties. Moreover, the mechanical properties and protease degradation characteristics that supported murine IMCD tubulogenesis in this study are different from those recently identified for human renal epithelial cells in heparin-based hydrogels (Weber et al., 2017), and suggest differences between these two epithelial cell sources. This fully synthetic matrix addresses major limitations of biological materials or hydrogels associated with lot-to-lot compositional and structural variability and tumor-derived nature that severely restrict scale-up applications and clinical translation. Furthermore, the modular nature of this hydrogel platform allows the characterization of the elementary matrix property contributions to renal organ development.

MATERIALS AND METHODS

Immunofluorescence analysis

Primary antibodies used were rabbit anti-laminin (1:50, L9393, Sigma-Aldrich), and mouse anti-MT1-MMP (5 µg/ml, IM57, Millipore) antibodies. Secondary antibodies used were goat anti-mouse-IgG conjugated to Alexa Fluor 647 (Thermo Fisher Scientific), mouse anti-rabbit-IgG conjugated to CFL 647 (sc-516251, Santa Cruz Biotechnology) and donkey anti-rabbit-IgG conjugated to Dylight 650 (84546, Thermo Fisher Scientific). Nuclei were stained with DAPI and actin was stained with Rhodamine–phalloidin (R415, Thermo Fisher Scientific). Gels were washed extensively in DPBS and fixed in 4% formaldehyde in DPBS for 20 min. Gels were incubated for 30 min in blocking buffer (1% bovine serum albumin, 1% goat serum, 0.1% fish skin gelatin, 0.5% Triton X-100 and 0.05% sodium azide in PBS). Samples were incubated in primary antibodies diluted in blocking buffer at 4°C overnight. Secondary antibodies, Rhodamine–phalloidin and nuclear stain (DAPI) were diluted in blocking buffer and incubated at 4°C overnight. Fluorescence images for tubule assessment were captured with 20×, 40×, 60× and 100× objectives in a Nikon Eclipse Ti microscope connected to a C2+ confocal module. Area and Feret diameter of multicellular IMCD structures were measured from fluorescence images of specimen cross sections through ImageJ macros. Morphological scoring was performed by a researcher blind to the experimental conditions and that was not involved in data acquisition. Relative fluorescence analysis was performed on *z*-stack fluorescent images stained for MT1-MMP using ImageJ macros.

Cell culture

Immortalized mouse inner medullary collecting duct (IMCD) cells [isolated from $\alpha v^{flox/flox}$ mice, as described previously (Zhang et al., 2009; Husted et al., 1988) were maintained in Dulbecco's modified Eagle's medium (DMEM)/Nutrient Mixture F-12 Ham (DMEM/F-12 50/50; D8437, Sigma-Aldrich)] supplemented with 10% fetal bovine serum (Life Technologies) and 1% antibiotic-antimycotic solution (MT-30-004-CI, MediaTech). Renal proximal tubule cells (RPTCs; isolated from $\beta 1^{flox/flox}$ mice, as described previously; Elias et al., 2014) were maintained in DMEM/F-12 (50/50 D8437, Sigma-Aldrich) supplemented with 2.5% fetal bovine serum (Life Technologies), 20 ng/ml hydrocortisone (H0135, Sigma-Aldrich), ITS medium supplement (5 µg/ml insulin-5 µg/ml transferrin-5 ng/ml selenite; I1884, Sigma-Aldrich), 6.7 mg/ml 3,3′,5-triiodo-L-thyronine (T5516, Sigma-Aldrich), 0.096 mg/ml D-valine (V1255, Sigma-Aldrich) and 100 µg/ml Normocin (ant-nr-2, InvivoGen). RPTCs were maintained at 33°C with 0.1% interferon γ (14777, Sigma-Aldrich) in culture medium during growth and expansion. At least 10 days before 3D encapsulation, RPTCs were cultured in absence of interferon γ at 37°C to induce differentiation.

Hydrogel formation and 3D cell encapsulation

PEG-4MAL hydrogels were prepared as described previously (Cruz-Acuña et al., 2018). Briefly, PEG-4MAL macromer (molecular mass of 22,000 or 11,000; Laysan Bio) was dissolved in 4-(2-hydroxyethyl)piperazine-1-ethanesulfonic acid (HEPES) buffer (20 mM in DPBS, pH 7.4). Adhesive and crosslinking peptides were custom synthesized by AAPPTec. Adhesive peptides RGD (GRGDSPC), GFOGER [GYGGGP(GPP)$_5$GFOGER (GPP)$_5$ GPC], YIGSR (CGGEGYGEGYIGSR) and RDG (GRDGSPC) were dissolved in HEPES at 10.0 mM (5× final ligand density) and mixed with PEG-4MAL at a 2:1 PEG-4MAL/ligand ratio to generate functionalized PEG-4MAL precursor. Bis-cysteine crosslinking peptides IPES (GCRDIPES↓LRAGDRCG; ↓denotes enzymatic cleavage site) or GPQ-W (GCRDGPQG↓IWGQDRCG), or non-degradable crosslinking molecules hexa(ethylene glycol) dithiol (PEGDT, 734616; Sigma-Aldrich) were dissolved in HEPES at a density corresponding to a 1:1 maleimide-to-cysteine ratio after accounting for maleimide groups reacted with adhesive peptide. Cells were resuspended at 5× final density in ice-cold serum-free medium and kept on ice. To form hydrogels, adhesive peptide-functionalized PEG-4MAL macromer, cells and crosslinking peptide were polymerized for 20 min before addition of complete growth medium. A final density of 75,000 cells/ml were encapsulated in all hydrogels. Matrigel™ encapsulation was performed as described previously (Giles et al., 2014). Briefly, cells were resuspended in culture medium at a density of 100,000 cells/ml and mixed with thawed Matrigel™ (354277, Corning) at a 1:1 Matrigel™–cell mixture ratio. A full growth medium change was performed every 2–3 days for all experiments. Sample size was established as at least four gels per condition with the premise that an outcome present in four different gels under a specific condition will reveal the population behavior for this given condition.

Hydrogel characterization

The storage and loss moduli of hydrogels were assessed by dynamic oscillatory strain and frequency sweeps performed on a MCR 302 stress-controlled rheometer (Anton Paar) with a 9-mm diameter, 2° cone and plate geometry. Oscillatory frequency sweeps were used to examine the storage and loss moduli (ω=0.5–100 rad s^{-1}) at a strain of 2.31%.

Viability and proliferation assays

For cell viability assessment, PEG-4MAL gels were incubated in 0.5% collagenase I (Worthington Biochemical), 0.5 µM C_{12}-Resazurin (LIVE; L34951, Thermo Fisher Scientific) and 1 µM TOTO-3 iodide (dead; T3604, Thermo Fisher Scientific) in serum-free medium until hydrogel was completely dissolved and cells settled at bottom of wells. Proliferation was assayed using the Click-iT EdU Imaging Kit (C10338, Thermo Fisher Scientific) following the manufacturer's instructions. EdU labeling was performed for 5.5 h at a final concentration of 10 µM. Samples were imaged with Nikon Plan Fluor 10× (NA 0.30) or Plan Fluor 20× (NA 0.45) objectives in a C2-Plus Confocal System (NIS Elements acquisition software). Cells were counted with ImageJ (NIH) macros.

Inhibition of mediators of mechanotransduction, MT1-MMP and integrin subunits

Inhibition of myosin II or Rho-associated kinases was performed by using blebbistatin (203389, Calbiochem) or Y-27632 (688002, Calbiochem), respectively, by adding 25 µM to the growth medium 5 days after cell encapsulation in hydrogel. Inhibition of the MT1-MMP catalytic domain was performed by adding 2 or 6 µg/ml of anti-MT1-MMP antibody (AB6005, Millipore) to the growth medium 3 days after cell encapsulation in hydrogel. Inhibition of integrin subunits α1, α2 or β1 was performed by adding 0.5 µg/ml of anti-rat/mouse CD49a (555001, BD Pharmingen), anti-rat/mouse CD49b (554998, BD Pharmingen) or AIIB2 (Developmental Studies Hybridoma Bank), respectively. Samples were imaged using a Nikon Eclipse Ti microscope connected to a C2+ confocal module.

Statistical analyses

Statistical analyses were performed using GraphPad Prism 6.0. For normally distributed data with equal variances, one-way ANOVA with Tukey's multiple comparison test was used, as well as unpaired *t*-tests with Welch's correction. For non-normally distributed data, Kruskal–Wallis with Dunn's multiple comparisons test was used. *P*-values of statistical significance are represented as ****P<0.0001, ***P<0.0002, **P<0.0021, *P<0.0332. P<0.05 was considered significant.

Acknowledgements
We thank Woojin M. Han (Woodruff School of Mechanical Engineering, Petit Institute for Bioengineering and Bioscience) for the scientific input and technical support.

Competing interests
The authors declare no competing or financial interests.

Author contributions
Conceptualization: R.C.-A., R.Z., A.J.G.; Methodology: R.C.-A., A.M.-R., R.Z.; Software: R.C.-A.; Formal analysis: R.C.-A., A.M.-R., A.Y.C.; Investigation: R.C., A.Y.C.; Resources: A.J.G.; Data curation: R.C.-A., A.M.-R.; Writing - original draft: R.C.-A.; Writing - review & editing: R.C.-A., A.M.-R., R.Z., A.J.G.; Visualization: R.Z., A.J.G.; Supervision: A.J.G.; Funding acquisition: A.J.G.

Funding
This research was supported by the National Institutes of Health (NIH) (R01 AR062368, R01 EB024322 to A.J.G. and 5-T32-EB006343-10 to A.M.R.), the National Science Foundation Graduate Research Fellowship (DGE-1650044 to R.C.-A.) and by the Alfred P. Sloan Foundation's Minority Ph.D. (MPHD) Program (G-2016-20166039 to R.C.-A.). Deposited in PMC for release after 12 months.

Supplementary information
Supplementary information available online at
http://jcs.biologists.org/lookup/doi/10.1242/jcs.226639.supplemental

References

Adams, J. C. and Watt, F. M. (1993). Regulation of development and differentiation by the extracellular matrix. *Development* **117**, 1183.
Caliari, S. R. and Burdick, J. A. (2016). A practical guide to hydrogels for cell culture. *Nat. Methods* **13**, 405-414. doi:10.1038/nmeth.3839
Chen, D., Roberts, R., Pohl, M., Nigam, S., Kreidberg, J., Wang, Z., Heino, J., Ivaska, J., Coffa, S., Harris, R. C. et al. (2004). Differential expression of collagen- and laminin-binding integrins mediates ureteric bud and inner medullary collecting duct cell tubulogenesis. *Am. J. Physiol. Renal Physiol.* **287**, F602-F611. doi:10.1152/ajprenal.00015.2004
Cruz-Acuña, R. and García, A. J. (2016). Synthetic hydrogels mimicking basement membrane matrices to promote cell-matrix interactions. *Matrix Biol.* **57-58**, 324-333. doi:10.1016/j.matbio.2016.06.002
Cruz-Acuña, R., Quirós, M., Farkas, A. E., Dedhia, P. H., Huang, S., Siuda, D., García-Hernández, V., Miller, A. J., Spence, J. R., Nusrat, A. et al. (2017). Synthetic hydrogels for human intestinal organoid generation and colonic wound repair. *Nat. Cell Biol.* **19**, 1326-1335. doi:10.1038/ncb3632
Cruz-Acuña, R., Quirós, M., Huang, S., Siuda, D., Spence, J. R., Nusrat, A. and García, A. J. (2018). PEG-4MAL hydrogels for human organoid generation, culture, and in vivo delivery. *Nat. Protoc.* **13**, 2102-2119. doi:10.1038/s41596-018-0036-3
Elias, B. C., Mathew, S., Srichai, M. B., Palamuttam, R., Bulus, N., Mernaugh, G., Singh, A. B., Sanders, C. R., Harris, R. C., Pozzi, A. et al. (2014). The integrin β1 subunit regulates paracellular permeability of kidney proximal tubule cells. *J. Biol. Chem.* **289**, 8532-8544. doi:10.1074/jbc.M113.526509
Emsley, J., Knight, C. G., Farndale, R. W. and Barnes, M. J. (2004). Structure of the integrin α2β1-binding collagen peptide. *J. Mol. Biol.* **335**, 1019-1028. doi:10.1016/j.jmb.2003.11.030
Enemchukwu, N. O., Cruz-Acuña, R., Bongiorno, T., Johnson, C. T., García, J. R., Sulchek, T. and García, A. J. (2016). Synthetic matrices reveal contributions of ECM biophysical and biochemical properties to epithelial morphogenesis. *J. Cell Biol.* **212**, 113-124. doi:10.1083/jcb.201506055
Giancotti, F. G. and Ruoslahti, E. (1999). Integrin signaling. *Science* **285**, 1028. doi:10.1126/science.285.5430.1028
Giles, R. H., Ajzenberg, H. and Jackson, P. K. (2014). 3D spheroid model of mIMCD3 cells for studying ciliopathies and renal epithelial disorders. *Nat. Protoc.* **9**, 2725. doi:10.1038/nprot.2014.181
Gjorevski, N., Ranga, A. and Lutolf, M. P. (2014). Bioengineering approaches to guide stem cell-based organogenesis. *Development* **141**, 1794-1804. doi:10.1242/dev.101048
Gjorevski, N., Sachs, N., Manfrin, A., Giger, S., Bragina, M. E., Ordóñez-Morán, P., Clevers, H. and Lutolf, M. P. (2016). Designer matrices for intestinal stem cell and organoid culture. *Nature* **539**, 560-564. doi:10.1038/nature20168
Hughes, C. S., Postovit, L. M. and Lajoie, G. A. (2010). Matrigel: a complex protein mixture required for optimal growth of cell culture. *Proteomics* **10**, 1886-1890. doi:10.1002/pmic.200900758
Husted, R. F., Hayashi, M. and Stokes, J. B. (1988). Characteristics of papillary collecting duct cells in primary culture. *Am. J. Physiol. Renal Physiol.* **255**, F1160-F1169. doi:10.1152/ajprenal.1988.255.6.F1160
Hynes, R. O. (2002). Integrins: bidirectional, allosteric signaling machines. *Cell* **110**, 673-687. doi:10.1016/S0092-8674(02)00971-6
Kikkawa, Y., Hozumi, K., Katagiri, F., Nomizu, M., Kleinman, H. K. and Koblinski, J. E. (2014). Laminin-111-derived peptides and cancer. *Cell Adhes. Migr.* **7**, 150-159. doi:10.4161/cam.22827
Kloxin, A. M., Kasko, A. M., Salinas, C. N. and Anseth, K. S. (2009). Photodegradable hydrogels for dynamic tuning of physical and chemical properties. *Science* **324**, 59-63. doi:10.1126/science.1169494
Lash, J. W., Linask, K. K. and Yamada, K. M. (1987). Synthetic peptides that mimic the adhesive recognition signal of fibronectin: differential effects on cell-cell and cell-substratum adhesion in embryonic chick cells. *Dev. Biol.* **123**, 411-420. doi:10.1016/0012-1606(87)90399-X
Lelongt, B. and Ronco, P. (2003). Role of extracellular matrix in kidney development and repair. *Pediatr. Nephrol.* **18**, 731-742. doi:10.1007/s00467-003-1153-x
Liu, Y., Chattopadhyay, N., Qin, S., Szekeres, C., Vasylyeva, T., Mahoney, Z. X., Taglienti, M., Bates, C. M., Chapman, H. A., Miner, J. H. et al. (2009). Coordinate integrin and c-Met signaling regulate Wnt gene expression during epithelial morphogenesis. *Development* **136**, 843-853. doi:10.1242/dev.027805
Livant, D. L., Brabec, R. K., Kurachi, K., Allen, D. L., Wu, Y., Haaseth, R., Andrews, P., Ethier, S. P. and Markwart, S. (2000). The PHSRN sequence induces extracellular matrix invasion and accelerates wound healing in obese diabetic mice. *J. Clin. Invest.* **105**, 1537-1545. doi:10.1172/JCI8527
Lo, A. T., Mori, H., Mott, J. and Bissell, M. J. (2012). Constructing three-dimensional models to study mammary gland branching morphogenesis and functional differentiation. *J. Mammary Gland Biol. Neoplasia* **17**, 103-110. doi:10.1007/s10911-012-9251-7
Lutolf, M. P. and Hubbell, J. A. (2005). Synthetic biomaterials as instructive extracellular microenvironments for morphogenesis in tissue engineering. *Nat. Biotechnol.* **23**, 47. doi:10.1038/nbt1055
Madl, C. M., Heilshorn, S. C. and Blau, H. M. (2018). Bioengineering strategies to accelerate stem cell therapeutics. *Nature* **557**, 335-342. doi:10.1038/s41586-018-0089-z
Miyamoto, S., Akiyama, S. and Yamada, K. M. (1995). Synergistic roles for receptor occupancy and aggregation in integrin transmembrane function. *Science* **267**, 883. doi:10.1126/science.7846531
Montesano, R., Schaller, G. and Orci, L. (1991). Induction of epithelial tubular morphogenesis in vitro by fibroblast-derived soluble factors. *Cell* **66**, 697-711. doi:10.1016/0092-8674(91)90115-F
O'Brien, L. E., Zegers, M. M. P. and Mostov, K. E. (2002). Building epithelial architecture: insights from three-dimensional culture models. *Nat. Rev. Mol. Cell Biol.* **3**, 531-537. doi:10.1038/nrm859
Patterson, J. and Hubbell, J. A. (2010). Enhanced proteolytic degradation of molecularly engineered PEG hydrogels in response to MMP-1 and MMP-2. *Biomaterials* **31**, 7836-7845. doi:10.1016/j.biomaterials.2010.06.061
Phelps, E. A., Enemchukwu, N. O., Fiore, V. F., Sy, J. C., Murthy, N., Sulchek, T. A., Barker, T. H. and García, A. J. (2012). Maleimide cross-linked bioactive PEG hydrogel exhibits improved reaction kinetics and cross-linking for cell encapsulation and in situ delivery. *Adv. Mater.* **24**, 64-70, 62. doi:10.1002/adma.201103574
Pohl, M., Sakurai, H., Bush, K. T. and Nigam, S. K. (2000). Matrix metalloproteinases and their inhibitors regulate in vitro ureteric bud branching morphogenesis. *Am. J. Physiol. Renal Physiol.* **279**, F891-F900. doi:10.1152/ajprenal.2000.279.5.F891
Riggins, K. S., Mernaugh, G., Su, Y., Quaranta, V., Koshikawa, N., Seiki, M., Pozzi, A. and Zent, R. (2010). MT1-MMP-mediated basement membrane remodeling modulates renal development. *Exp. Cell Res.* **316**, 2993-3005. doi:10.1016/j.yexcr.2010.08.003
Rosines, E., Johkura, K., Zhang, X., Schmidt, H. J., Decambre, M., Bush, K. T. and Nigam, S. K. (2010). Constructing kidney-like tissues from cells based on programs for organ development: toward a method of in vitro tissue engineering of the kidney. *Tissue Eng. A* **16**, 2441-2455. doi:10.1089/ten.TEA.2009.0548
Sakurai, H., Barros, E., Tsukamoto, T., Barasch, J. and Nigam, S. (1997). An in vitro tubulogenesis system using cell lines derived from the embryonic kidney shows dependence on multiple soluble growth factors. *Proc. Natl. Acad. Sci. USA* **94**, 6279-6284. doi:10.1073/pnas.94.12.6279
Straight, A. F., Cheung, A., Limouze, J., Chen, I., Westwood, N. J., Sellers, J. R. and Mitchison, T. J. (2003). Dissecting temporal and spatial control of cytokinesis with a myosin II inhibitor. *Science* **299**, 1743-1747. doi:10.1126/science.1081412
Turk, B. E., Huang, L. L., Piro, E. T. and Cantley, L. C. (2001). Determination of protease cleavage site motifs using mixture-based oriented peptide libraries. *Nat. Biotechnol.* **19**, 661. doi:10.1038/90273
Uehata, M., Ishizaki, T., Satoh, H., Ono, T., Kawahara, T., Morishita, T., Tamakawa, H., Yamagami, K., Inui, J., Maekawa, M. et al. (1997). Calcium sensitization of smooth muscle mediated by a Rho-associated protein kinase in hypertension. *Nature* **389**, 990-994. doi:10.1038/40187
Weber, H. M., Tsurkan, M. V., Magno, V., Freudenberg, U. and Werner, C. (2017). Heparin-based hydrogels induce human renal tubulogenesis in vitro. *Acta Biomater.* **57**, 59-69. doi:10.1016/j.actbio.2017.05.035
Werb, Z., Tremble, P. M., Behrendtsen, O., Crowley, E. and Damsky, C. H. (1989). Signal transduction through the fibronectin receptor induces collagenase and stromelysin gene expression. *J. Cell Biol.* **109**, 877. doi:10.1083/jcb.109.2.877

Wickström, S. A., Radovanac, K. and Fässler, R. (2011). Genetic Analyses of Integrin Signaling. *Cold Spring Harbor Perspect. Biol.* **3**, a005116. doi:10.1101/cshperspect.a005116

Yu, W., Datta, A., Leroy, P., O'brien, L. E., Mak, G., Jou, T.-S., Matlin, K. S., Mostov, K. E. and Zegers, M. M. P. (2005). β1-integrin orients epithelial polarity via Rac1 and laminin. *Mol. Biol. Cell* **16**, 433-445. doi:10.1091/mbc.E04-05-0435

Zent, R., Bush, K. T., Pohl, M. L., Quaranta, V., Koshikawa, N., Wang, Z., Kreidberg, J. A., Sakurai, H., Stuart, R. O. and Nigám, S. K. (2001). Involvement of laminin binding integrins and laminin-5 in branching morphogenesis of the ureteric bud during kidney development. *Dev. Biol.* **238**, 289-302. doi:10.1006/dbio.2001.0391

Zhang, X., Mernaugh, G., Yang, D.-H., Gewin, L., Srichai, M. B., Harris, R. C., Iturregui, J. M., Nelson, R. D., Kohan, D. E., Abrahamson, D. et al. (2009). β1 integrin is necessary for ureteric bud branching morphogenesis and maintenance of collecting duct structural integrity. *Development* **136**, 3357. doi:10.1242/dev.036269